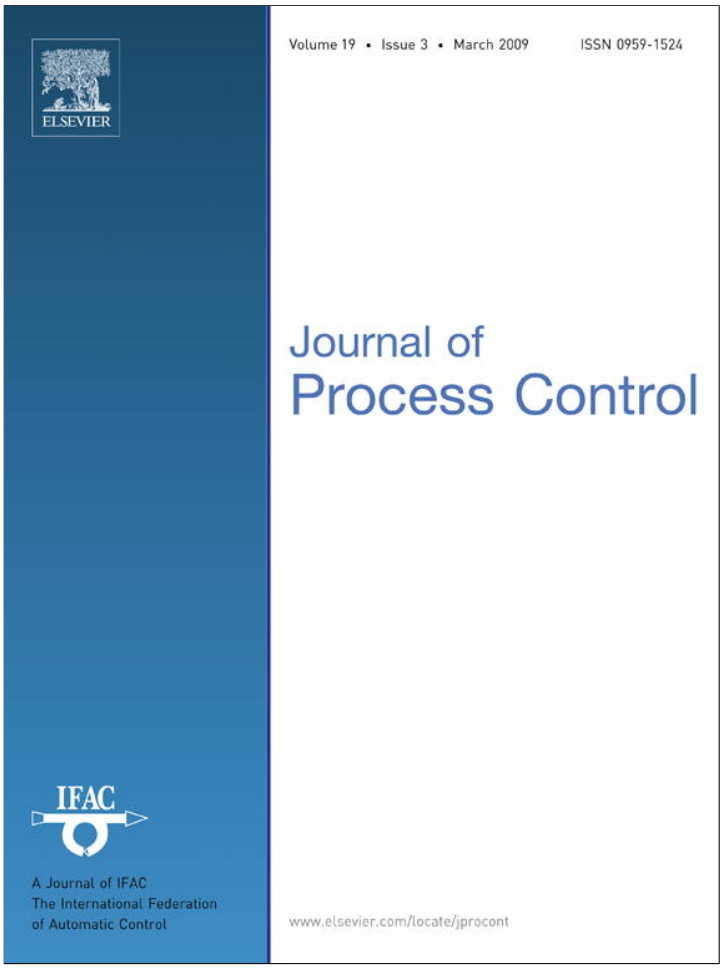

Journal of Process Control 19 (2009) 433–442

Contents lists available at ScienceDirect

Journal of Process Control

journal homepage: www.elsevier.com/locate/jprocont

Model-predictive control of feed flow reversal in a reverse osmosis desalination process

Alex R. Bartman, Charles W. McFall, Panagiotis D. Christofides *, Yoram Cohen

Department of Chemical and Biomolecular Engineering, University of California, 5531 Boelter Hall, Los Angeles, CA 90095-1592, United States

ARTICLE INFO

Article history:
Received 19 December 2007
Received in revised form 18 June 2008
Accepted 18 June 2008

Keywords:
High-recovery reverse-osmosis desalination
Model-predictive control
Flow reversal

ABSTRACT

Model-predictive control algorithms are applied to a high capacity reverse osmosis (RO) membrane desalination process simulation that utilizes feed flow reversal in order to prevent and/or reverse scale crystal formation on the membrane surface. A dynamic non-linear model which incorporates feed concentration and membrane properties is used for simulation and demonstration of optimally controlled feed flow reversal. Before flow reversal can take place on a high capacity RO plant, the flow into the membrane unit must be carefully reduced to eliminate the risk of membrane module damage and unnecessary energy consumption. A cost function is formulated for the transition between the normal high flow steady-state operating point to a low flow steady-state operating point where it is safe to reverse the flow direction. Open-loop and closed-loop simulations demonstrate non-linear model-predictive control strategies that induce transition from the high-flow to low-flow steady-states in an optimal way while subjected to plant-model mismatch on the feed concentration, actuator magnitude and rate constraints, and sampled measurements.

1. Introduction

Reverse osmosis (RO) membrane desalination has emerged as one of the leading methods for water desalination due to the low cost and energy efficiency of the process [17]. Lack of fresh water sources has necessitated further development of these desalination plants, especially in areas with dry climates. In many reverse osmosis processes, particularly with brackish water feeds or processes running at a high level of recovery, dissolved ions can precipitate out of solution and crystallize on the membrane surface in a process called scaling. Scale formation on the membrane surface will lead to decreased permeate productivity [7], as well as permanent membrane damage if scaling is allowed to progress past its initial stages.

Several methods are currently used to prevent scale formation; addition of anti-scalant chemicals to the feed or flushing the membrane units with low-TDS (total dissolved solids) permeate water. These current methods of scale mitigation have several disadvantages. Anti-scalants are only useful to a degree, and if added in excess, may actually promote scaling or fouling [18]. The cost of the anti-scalant compounds is also an important consideration [3]. In the case of the permeate flush, this process will require the reverse osmosis operation to stop for a substantial amount of time to allow for the flushing cycle, eliminating any permeate production (even using up some of the previously produced permeate water). To deal with these issues, a novel technique called feed flow reversal has been developed, which can prevent scale formation without the addition of expensive chemicals or extensive periods of system down-time [16]. This technique uses a system of solenoid valves around the membrane modules configured specifically so that the direction of the feed flow through the membrane units can be reversed (see Fig. 1). This reversal of the feed flow also reverses the axial salt concentration profile [6] at the surface of the membrane, effectively "resetting the induction clock", where induction refers to the amount of time before scale crystals begin to form on the membrane surface [16]. The reversal, if activated after crystals have already been formed, also allows the dissolution of a substantial portion of scale deposited on the membrane surface.

It is imperative to operate the flow reversal process for the correct length of time; switching back to normal flow too quickly may leave scale crystals on the membrane (and in the case where scale crystals have not formed yet, the induction clock will not "reset"), while operating the flow reversal for too long may cause scale to form on the outlet end of the membrane surface. Several techniques can be employed to determine if scale has formed; measurements of the permeate flow can be monitored to determine if flux decline has occurred, or a novel method such as the EX-situ Scale Observation Detector (EXSOD) system can be used [19]. With the latter method, scale crystals can be detected before flux decline occurs via automated image analysis software (currently under development by the authors); this algorithm is also able to trigger the switch between normal flow and flow reversal mode.

* Corresponding author. Tel.: +1 310 794 1015; fax: +1 310 206 4107.
E-mail address: pdc@seas.ucla.edu (P.D. Christofides).

0959-1524/$ - see front matter © 2008 Elsevier Ltd. All rights reserved.
doi:10.1016/j.jprocont.2008.06.016

When operating a system that utilizes feed flow reversal, it is important to carry out the mode switching (from forward flow to reverse flow) in a manner which will not cause water hammer. The phenomenon of water hammer takes place when fluid moving at a moderate to high velocity (velocity > 1.5 m/s for the example in this work) suddenly encounters a blockage in the pipe (for instance, when a solenoid valve is instantly closed). The fluid's inertia causes it to slam into the blockage, causing a pressure wave and often wear/damage to the process equipment [8]. The Joukowski formula [15] can be used to estimate the magnitude of the pressure wave caused by water hammer for a given system configuration, and it is seen that this problem can be especially prominent in large systems with a high feed flow rate.

For example, consider the system presented in Fig. 2. Initially solenoid valves s_2 and s_3 are closed and s_1 and s_4 are open. Furthermore, the velocity entering the membrane unit, v_{fr}, is 10 m/s. When flow reversal is initiated, solenoid valves s_2 and s_3 are opened and assuming similar flow resistance in each path, the flow splits approximately evenly through the three possible paths. The flows through s_2, s_3, and the membrane unit are approximately 3.3 m/s. However, the flow going through s_1 and s_4 is approximately 6.7 m/s. With a maximum velocity threshold of 1.5 m/s, none of these flow velocities are low enough to enable the closure of a solenoid valve without the possibility of causing component damage through water hammer. From this example, it is clear that with the configuration seen in Fig. 2, water hammer is of concern when the velocity into the membrane units is approximately 1.5 times the water hammer threshold.

Motivated by these considerations, the goal of this work is to use model-predictive control (MPC) to determine the optimal switching path from normal operating conditions to a condition where the stream velocity entering the membranes is much lower; preventing water hammer during solenoid valve closure while avoiding pressure fluctuations and decreased process performance during the transition. Alleviating these phenomena will prolong equipment life-span and help to maximize the productivity of the RO system. The formulation presented in this work is specific to the system presented in Fig. 2, but it is important to note that these MPC algorithms can be adapted to any flow reversal equipped reverse osmosis system where the operator is able to control the stream velocity entering the membrane units. Model-predictive control has not been employed for use with the feed flow reversal technique, but has been evaluated for the overall control of RO desalination processes [1]. It is noted that in a recent work [11], Lyapunov-based non-linear control systems and model-based monitoring schemes were designed for fault-tolerant control of RO processes in the presence of actuator faults without dealing with the issue of optimization of the feed flow reversal process. Optimization with MPC requires the use of a RO desalination system model, which has been derived based on mass and energy balances [10]. A cost function that takes into account control action, stream velocities, and system pressure is proposed, along with several hard process constraints which represent physical limitations of the system. The model, cost function, and constraints are arranged into a non-linear optimization problem which is solved through the use of a numerical optimization algorithm. Closed-loop simulations with MPC are performed in this work to demonstrate the mode switching dynamics. The MPC algorithm is also applied to the system when a plant-model mismatch on feed concentration is imposed. This plant-model mismatch will allow for evaluation of the disturbance rejection by the controller when using feedback from the plant model.

2. RO system model

As seen in Fig. 2, feed water enters the system and is pressurized by the high-pressure pump. The pressurized stream is split into a bypass stream (with velocity v_b) and the stream which enters the spiral-wound membrane unit(s) (v_{fr}). Two streams also exit the membrane module, the retentate (or brine) stream, with velocity v_r, and the permeate stream. The downstream pressure of all of the exit streams is assumed to be atmospheric pressure.

The model derivation is based on an overall mass balance and local energy balances around the valves of the system [10]. In

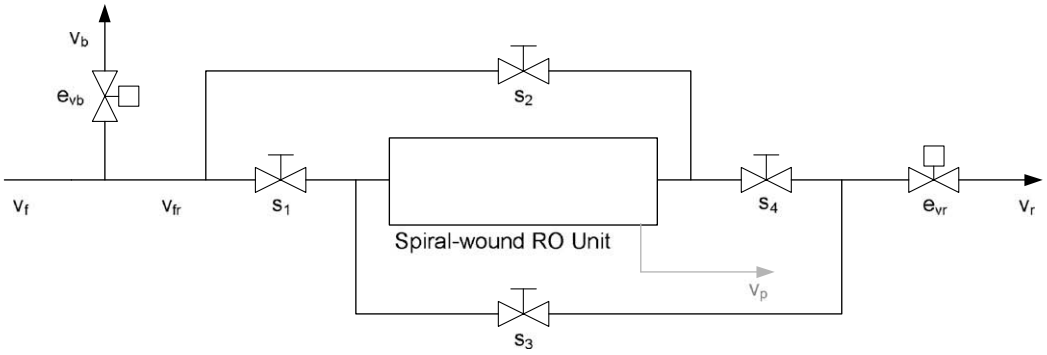

Fig. 1. An expanded view the flow reversal configuration surrounding the spiral-wound unit.

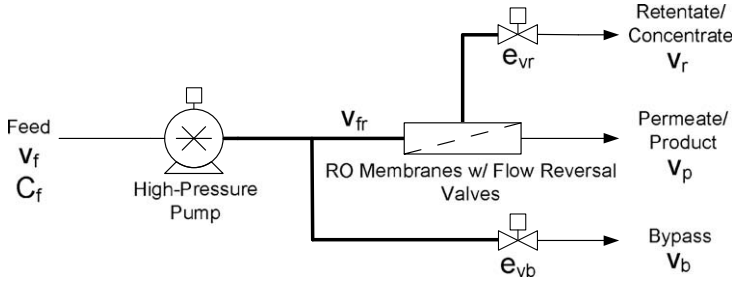

Fig. 2. Overall reverse osmosis system diagram.

the model derivation, it is assumed that the water is incompressible, all components are operated on the same plane (potential energy terms due to gravity are neglected), and the density of the water is assumed to be constant. It is also assumed that the effective concentration in the RO unit is a weighted average of the feed and retentate concentrations (Eq. (4)).

The model derivation results in two non-linear ordinary differential equations (ODEs), along with an algebraic expression for system pressure. An equation for the osmotic pressure based on the temperature and effective concentration in the membrane unit was developed in [9], and is used as an estimate for various solutions. Specifically, the model has the following form:

$$\frac{dv_b}{dt} = \frac{A_p^2}{A_m K_m V}(v_f - v_b - v_r) + \frac{A_p}{\rho V}\Delta\pi - \frac{1}{2}\frac{A_p e_{vb} v_b^2}{V} \quad (1)$$

$$\frac{dv_r}{dt} = \frac{A_p^2}{A_m K_m V}(v_f - v_b - v_r) + \frac{A_p}{\rho V}\Delta\pi - \frac{1}{2}\frac{A_p e_{vr} v_r^2}{V} \quad (2)$$

$$\Delta\pi = \delta C_{eff}(T + 273) \quad (3)$$

$$C_{eff} = C_{feed}\left(a + (1-a)\left(\frac{(1-R) + R(v_f - v_b)}{v_r}\right)\right) \quad (4)$$

$$P_{sys} = \frac{\rho A_p}{A_m K_m}(v_f - v_b - v_r) + \Delta\pi \quad (5)$$

where ρ is the fluid density, V is the system volume, v_f is the feed velocity, A_p is the pipe cross-sectional area, A_m is the membrane area, K_m is the membrane overall mass transfer coefficient, C_f is the amount of total dissolved solids (TDS) in the feed, a is an effective concentration weighting coefficient, δ is a constant relating effective concentration to osmotic pressure, v_b is the bypass flow velocity, v_r is the retentate flow velocity, P_{sys} is the system pressure, R is the fractional salt rejection of the membrane, e_{vb} is the bypass valve resistance, and e_{vr} is the retentate valve resistance. Using these dynamic equations, various control techniques can be applied using the valve resistance values as the manipulated inputs (e_{vb}, e_{vr}). At very small valve resistance values, the valve behaves as an open pipe; as the valve resistance becomes very large, the valve behaves as a total obstruction and the flow velocity goes to zero [2].

In order to accurately model the valve dynamics and obtain practical constraints, the concept of valve C_v is used. The definition of C_v for a valve in a water system is presented in Eq. (6), where Q is the volumetric flow rate through the valve.

$$C_v = \frac{Q}{\sqrt{P_{sys}}} \quad (6)$$

Using a simplified energy balance around one valve:

$$\frac{dv}{dt} = \frac{P_{sys} A_p}{\rho V} - \frac{1}{2}\frac{A_p e_v v^2}{V} \quad (7)$$

Steady-state is assumed, and the simplified energy balance is rearranged to yield:

$$C_v = \frac{1}{A_p\sqrt{\frac{1}{2}\rho e_v}} \quad (8)$$

Depending on the type of valve and its flow characteristics, it is assumed that the C_v value (and in turn, the e_v values from the model) can be related to the valve position (percentage open) through the following logarithmic relation based on commercially available valve data:

$$O_p = \mu \ln\left(\frac{1}{A_p\sqrt{\frac{1}{2}\rho e_v}}\right) + \phi \quad (9)$$

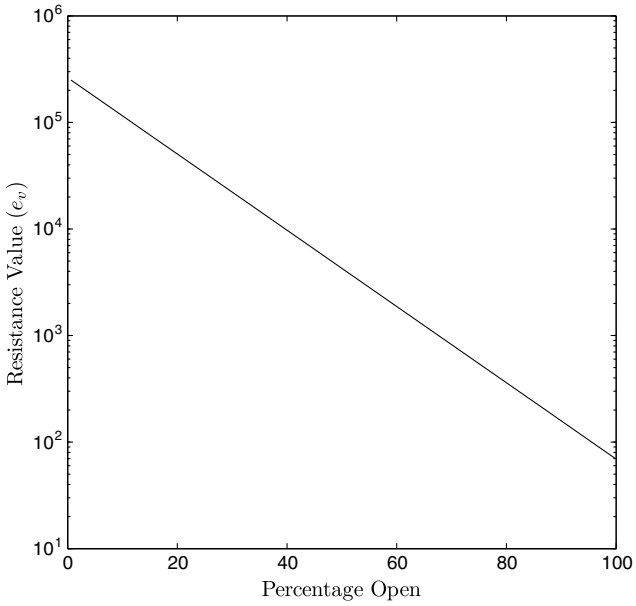

Fig. 3. Valve resistance values (e_v) vs. valve position.

where μ and ϕ are constants depending on the valve properties. For the model presented in this paper, the curve relating valve position (O_p) to resistance value (e_v) is shown in Fig. 3. It can be seen in Fig. 3 that as the valve position goes to zero (fully closed), the valve resistance values begin to grow at an increasing rate; and as the valve approaches the fully-open position, the resistance values change slowly. This treatment of the valve characteristics allows for constraints based on valve actuator speed to be incorporated into the RO system model and into the controller calculations.

3. Model-predictive control of flow reversal

When switching the system into flow reversal mode, it is desired to bring the feed velocity into the membranes (v_{fr}) below the velocity threshold; where the flow will not cause significant water hammer when the solenoid valves are closed. In order to decrease the membrane feed velocity (v_{fr}), it will be necessary to open the bypass valve. It is desired to keep the system pressure constant while decreasing the velocity so that the membrane and system components will not be damaged. This can be done by closing the retentate valve while the bypass valve is being opened, in such a fashion that the system pressure fluctuates less than a pre-defined tolerance. MPC is used to complete this transition in an optimal way.

When reversing the flow, the solenoid valves (s_i), arranged as seen in Fig. 1, are opened/closed in a specific sequence. First, valves s_2 and s_3 are opened, then valves s_1 and s_4 are closed. After these actions are completed, the retentate and bypass valves can be manipulated to return the process to the desired steady-state. The normal steady-state operating point is used as the initial condition for the mode switching. To determine the final state after mode switching, the procedure is as follows: Using the normal steady-state operating point, the pressure set point is calculated using Eq. (5). In this case, $P_{sys}^{sp} = 457.51$ psi. Second, setting the bypass velocity to $v_f - 1.5$ m/s (equivalent to setting $v_{fr} = 1.5$ m/s) and using the desired pressure set point, the low-flow steady-state operating point value for v_r^{lss} can be determined. With the steady-state values of v_r^{lss}, v_b^{lss}, and the pressure set point P_{sys}^{sp}, the model equations can be solved for the valve resistance values e_{vb}^{lss} and e_{vr}^{lss} corresponding to the low-flow operating point. Following this procedure, the low-flow steady-state operating point is known,

but the optimal path taken to get there from the initial operating steady-state is not.

While it is desired to complete this flow direction switching with minimal impact on the system pressure, and in the shortest time possible, it is also necessary to factor in several system parameters such as pressure variation allowed, the bypass stream velocity as compared to the water hammer threshold, and the amount of control energy expended. To account for these issues, an optimization cost function is first proposed:

$$C(x,x_0,u)=\sum_{i=n_c}^{n_c+N}\left[\alpha\left(\frac{P_{sys}(i)}{P_{sys}^{sp}}-1\right)^2+\beta\left(\frac{v_{fr}(i)}{v_{wh}}-1\right)^2+\gamma\left(\left(\frac{e_{vb}(i)}{e_{vb}^{lss}}-1\right)^2+\left(\frac{e_{vr}(i)}{e_{vr}^{lss}}-1\right)^2\right)\right] \quad (10)$$

where n_c is the current time-step, n_c+N is the current time-step plus the prediction horizon, and v_{wh} is the water hammer threshold velocity. The prediction horizon, N, is defined such that the optimization is performed from the current time-step to N time-steps in the future (i.e., from $t=t_{current}$ to $t=t_{current}+Nt_{step}$).

The values of the cost function of Eq. (10) depend on the initial state of the system (x_0) and the state of the system between $t(n_c)$ and $t(n_c+N)$ (the state, x, is comprised of v_b and v_r). The cost function also depends heavily on the control actions used (u), and weights given to the individual terms by the weighting coefficients α, β, and γ. As the optimization procedure is carried out, the optimization algorithm allows for a set of non-linear constraints to be employed. In this formulation, the following two hard actuator constraints are enforced:

$$O_{pi}\geqslant 0 \quad (11)$$

$$\left|\frac{dO_{pi}}{dt}\right|\leqslant R_{valve}^{max} \quad (12)$$

The first constraint forces the valve position values to be positive, since negative values of this variable would be physically meaningless. The second constraint sets a maximum rate of opening/closing for the valves, R_{valve}^{max}. Additional constraints can be added; constraints on maximum system pressure or other system variables may be desirable for certain types of RO operations.

In order to optimize the constrained transition from normal flow to low-flow and incorporate feedback into the calculation of the control action, a non-linear model-predictive control (MPC) formulation is implemented [4,5,13,14]. In this method, a time frame for the transition is chosen, $t=0$ to $t=t_f$, along with an optimization time-step t_{step} and a prediction horizon N. Using these optimization parameters and the constraints along with the RO system model and the cost function weighting parameters α, β, and γ, the MPC control scheme can determine an optimal pair of control inputs, e_{vb} and e_{vr}, for each time-step.

The MPC optimization involves the following procedure:

1. The initial state vector and initial control value guesses are passed to a non-linear optimization algorithm based on sequential quadratic programming.
2. The optimization algorithm numerically integrates the model equations from $t=t_{current}$ to $t=t_{current}+Nt_{step}$ using the initial state vector and control value guesses.
3. The resulting state vector is used to calculate the value of the cost function.
4. A new set of control inputs are determined, and steps 2–4 are repeated until a minimum cost value is found (i.e., $\min_{e_{vb},e_{vr}} C(x,x_0,u)$) subject to the constraints of Eqs. (11) and (12).
5. Optimal control inputs for each t_{step} are made available to the controller and actuators.
6. Only the first of the optimal control inputs, $u(t_{current})$, is applied; the system of Eqs. (1) and (2) is numerically integrated for one time-step (from $t=t_{current}$ to $t=t_{current}+t_{step}$) using the first optimal control value to yield a new initial state for the next optimization.
7. The remaining optimal control values for the prediction horizon are used as an initial guess for the computation of the control values in the next step.
8. All steps are repeated for each optimization time-step from $t=0$ to $t=t_f-t_{step}$.

As implicitly stated above, all control values are applied in a sample-and-hold fashion; that is, a control value used in the integration on the interval $[t_{step_{n-1}}\ t_{step_n})$ is held constant over the entire interval, and then a new control value is determined by the optimization for the interval $[t_{step_n}\ t_{step_{n+1}})$.

4. Simulation results

4.1. Overview

In order to test the feasibility of MPC for feed flow reversal in a reverse osmosis desalination system, several simulation studies were carried out. Initially, it was desired to examine the effect of using the model-predictive controller to switch between steady-states when the process conditions are identical to the nominal plant model. Using a sampling time approximately one tenth of the system step response time, the model-predictive control formulation is applied to the system with various prediction horizons. These simulations are subsequently compared to an "open-loop manually controlled" transition where the control inputs are manipulated to their final values at the maximum rate allowed by the constraints, as well as the case where the transition is controlled using proportional–integral (PI) control.

Next, it was desired to simulate the switching between steady-states in the presence of a plant-model mismatch on the feed TDS value. The controller receives state feedback from the plant model at the end of each time-step (i.e., measurements of v_b and v_r), but an offset in system pressure and stream velocity is observed due to the mismatched MPC controller. Simulations are conducted at several prediction horizons, and an integral control input is applied after the MPC reaches steady-state in order to bring the system pressure back to the nominal pressure set point; see Table 1.

Finally, due to the relatively fast time scale of the system dynamics, the use of a steady-state approximation of the dynamic model equations (Eqs. (1) and (2)) was also investigated in the

Table 1
Process parameters and normal mode steady-state values (nss)

ρ = 1000	kg/m^3
V = 0.04	m^3
v_f = 10	m/s
A_p = 1.27	cm^2
A_m = 30	m^2
K_m = 9.218×10^{-9}	s/m
C_f = 10,000	mg/L
a = 0.5	
T = 25	°C
R = 0.993	
μ = 24.270	
ϕ = 153.554	
δ = 0.2641	Pa/(ppm*K)
v_b^{nss} = 1.123	m/s
v_r^{nss} = 4.511	m/s
P_{sys}^{sp} = 457.51	psi
e_{vb}^{nss} = 5000	
e_{vr}^{nss} = 310	

non-linear MPC formulation. Simulation results evaluating the effectiveness of this approach are presented.

4.2. Optimal mode transition without plant-model mismatch

As described in the overview, the first simulations demonstrate the switching to low-flow mode using model-predictive control (MPC) in the case where the controller model and plant model are identical. The controller uses measurements of the retentate and bypass stream velocities (system states) and manipulates the valve resistance values. In these simulations, the optimization parameters were set as shown in Table 2. Additionally, the system was simulated for 10 s (t_f), and the prediction horizon, N, was varied in each simulation. The results are presented in Figs. 4–6.

It can be seen that in the valve position and stream velocity plots (Figs. 5 and 6), only a small difference is observed between simulations with various prediction horizons. Even though the difference in control action is slight, a large effect is seen on the system pressure, seen in Fig. 4. In the case of the smallest prediction horizon ($N = 1$), the system pressure drops by approximately 55 psi before returning to the set point. It is seen that as the prediction horizon increases, the maximum deviation from the system pressure set point decreases, showing that the model-predictive control horizon is instrumental in minimizing pressure fluctuations.

The benefits of implementing MPC on the system pressure can be seen even more clearly when the optimized cases are compared to the "open-loop manually controlled" pressure in Fig. 7, where the valves are adjusted to their final steady-state at the maximum rate allowable by the constraints. In this case, a 100 + psi pressure variation caused by the "open-loop manually controlled" operation is observed; about two times larger than the one under MPC. Of course, the acceptable pressure deviation during mode transition depends on the specific RO process under consideration. However, the proposed MPC approach to addressing this control problem is flexible enough to allow for variation in the acceptable pressure level. Furthermore, it is important to point out that one can

Table 2
Optimization parameters and low-flow mode steady-state values (lss)

$t_0 = 0$	s
$t_{step} = 0.1$	s
$\alpha = 10{,}000$	
$\beta = 100$	
$\gamma = 200$	
$v_{wh} = 1.5$	m/s
$v_b^i = 1.123$	m/s
$v_r^i = 4.511$	m/s
$C_{feed}^c = 10{,}000$	ppm
$R_{max} = 10$	%/s
$v_b^{lss} = 8.5$	m/s
$v_r^{lss} = 0.267$	m/s
$P_{sys}^{sp} = 457.51$	psi
$e_{vb}^{lss} = 87.322$	
$e_{vr}^{lss} = 88{,}592$	

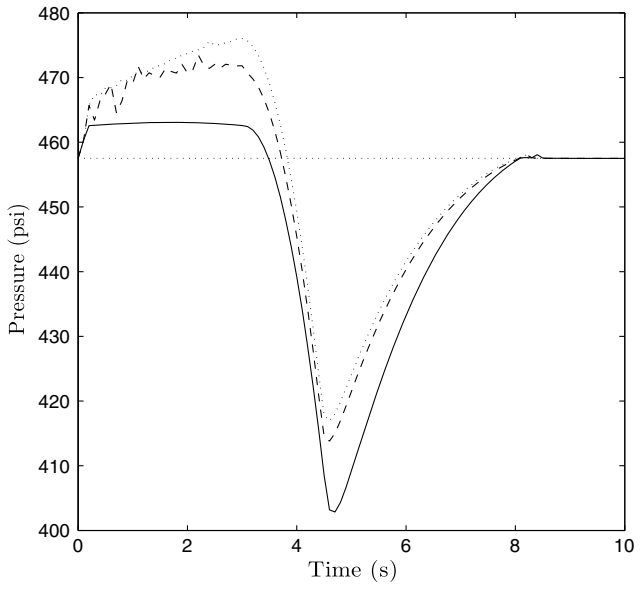

Fig. 4. Steady-state switching using MPC in the absence of plant-model mismatch: system pressure vs. time for $N = 1$ (solid line), $N = 3$ (dashed line), and $N = 5$ (dotted line), including pressure set point (horizontal line).

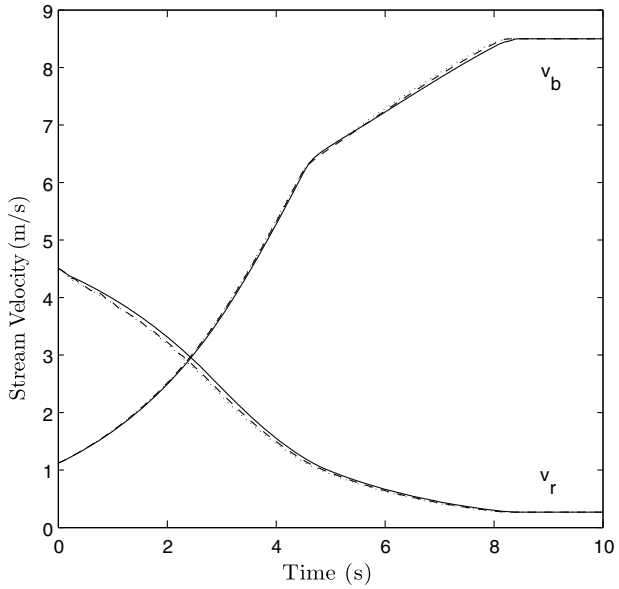

Fig. 5. Steady-state switching using MPC in the absence of plant-model mismatch: retentate and bypass stream velocities vs. time for $N = 1$ (solid line), $N = 3$ (dashed line), and $N = 5$ (dotted line).

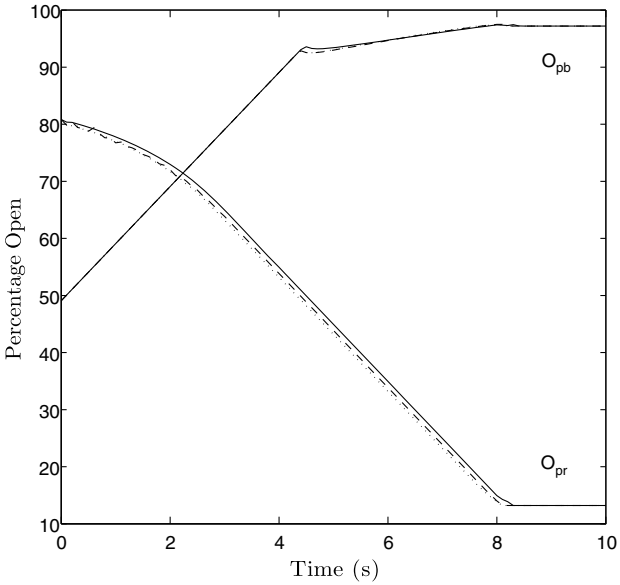

Fig. 6. Steady-state switching using MPC in the absence of plant-model mismatch: valve positions vs. time for $N = 1$ (solid line), $N = 3$ (dashed line), and $N = 5$ (dotted line).

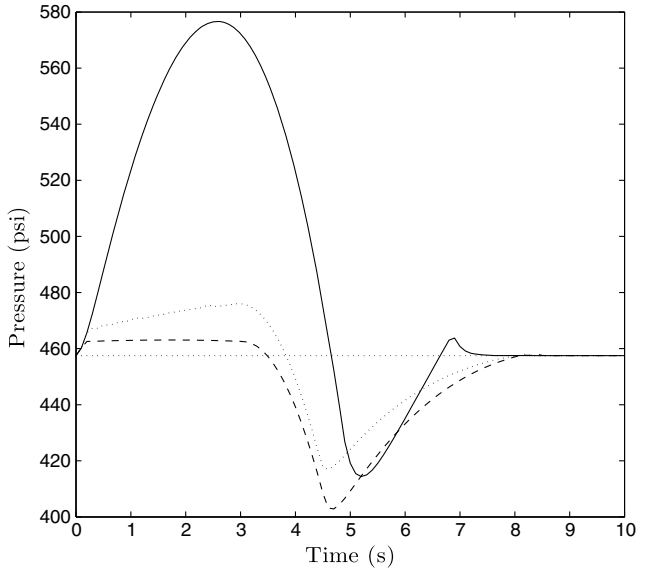

Fig. 7. Steady-state switching using MPC in the absence of plant-model mismatch: system pressure vs. time for "open-loop manually controlled" case (solid line), $N = 1$ (dashed line), and $N = 5$ (dotted line), including pressure set point (horizontal line.)

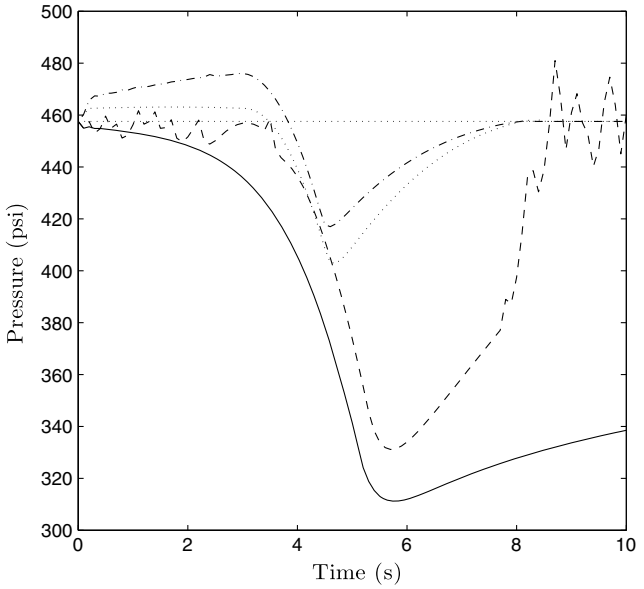

Fig. 8. Steady-state switching using MPC and PI in the absence of plant-model mismatch: pressure vs. time for first PI approach (dashed line), second PI approach (solid line), $N = 1$ (dotted line), and $N = 5$ (dash-dotted line), including pressure set point (horizontal line).

formulate "hard" constraints on the pressure in the optimization formulation of the MPC instead of penalizing the pressure deviation in the cost function (which is a "soft" constraint formulation) at the expense of restricting the feasibility region of the optimization problem.

It was also desired to compare the performance of the MPC to proportional–integral (PI) control. Two PI loops were implemented, one loop measuring the bypass stream velocity and using the bypass valve resistance to bring the bypass stream velocity to the water hammer threshold, and another loop measuring the system pressure while adjusting the retentate valve to maintain the system pressure at the set point. These two loops can be represented as follows:

$$u_{\mathrm{PI}}^{r} = K_{\mathrm{r}}(P_{\mathrm{sys}} - P_{\mathrm{sys}}^{\mathrm{sp}}) + \frac{1}{\tau_{\mathrm{r}}}\int_{0}^{t_{\mathrm{c}}}(P_{\mathrm{sys}} - P_{\mathrm{sys}}^{\mathrm{sp}})\mathrm{d}t \tag{13}$$

$$u_{\mathrm{PI}}^{b} = K_{\mathrm{b}}(v_{\mathrm{b}} - v_{\mathrm{b}}^{\mathrm{lss}}) + \frac{1}{\tau_{\mathrm{b}}}\int_{0}^{t_{\mathrm{c}}}(v_{\mathrm{b}} - v_{\mathrm{b}}^{\mathrm{lss}})\mathrm{d}t \tag{14}$$

Numerous closed-loop simulations were carried out under various PI controller tunings in order to determine the best achievable closed-loop responses. The best achievable closed-loop responses under two different approaches are presented: in the first approach, the PI parameters ($K_{\mathrm{r}} = -30$, $K_{\mathrm{b}} = 1000$, $\tau_{\mathrm{r}} = -30$, $\tau_{\mathrm{b}} = 1000$) were chosen so that the transition is accomplished in a comparable amount of time to the MPC controlled case. It is observed that this case has a poor transient closed-loop performance, due to the presence of large oscillations. It is also noted that the integral term of the PI controller is switched off when the control action is saturated (reaches maximum rate constraint or valve position reaches 100%) to mitigate the effect of integrator wind-up in the closed-loop system. In the second tuning approach, the PI parameters ($K_{\mathrm{r}} = -5$, $K_{\mathrm{b}} = 800$, $\tau_{\mathrm{r}} = -20$, $\tau_{\mathrm{b}} = 500$) were chosen in order to conduct the fastest response that does not exhibit any oscillations during the transition between the original and final steady-states. In this case, the pressure drops significantly more than any of the MPC cases, and takes a much longer time to converge back to the steady-state. The results can be seen in Figs. 8, 9. The comparisons of MPC with PI demonstrate that under the MPC formulation, the pressure will deviate from the set point less

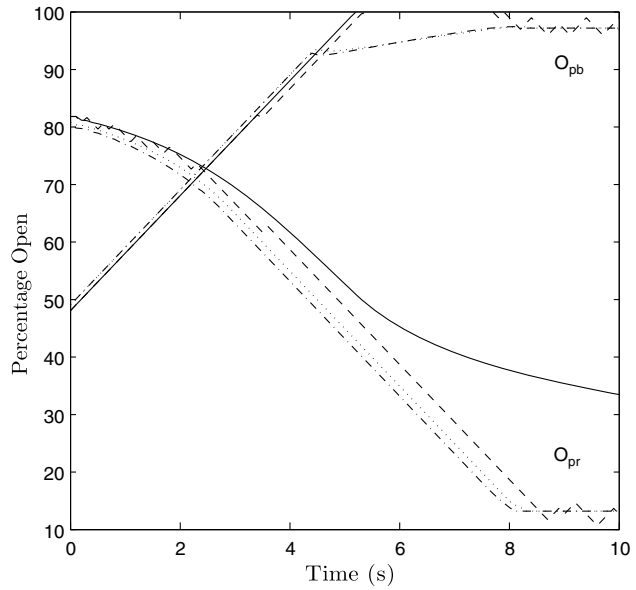

Fig. 9. Steady-state switching using MPC and PI in the absence of plant-model mismatch: valve positions vs. time for first PI approach (dashed line), second PI approach (solid line), $N = 1$ (dotted line), and $N = 5$ (dash-dotted line).

than the PI controlled case regardless of the PI tuning parameters. The MPC also provides a smoother transition which is accomplished in less time.

In Fig. 10, it can be observed that the values of the cost function decrease with increasing prediction horizon. The costs of these MPC controlled transitions fall between a lower and upper bound; if the pressure weighting in the cost function is set to zero (that is, the pressure is allowed to deviate with no penalty) and transition speed becomes the only factor in switching steady-states, then the valves will be opened and closed as fast as possible (equivalent to the "open-loop manually controlled" case). This situation leads to a lower bound on the achievable cost since all of the MPC controlled cases are penalized by pressure fluctuations. In the opposite situa-

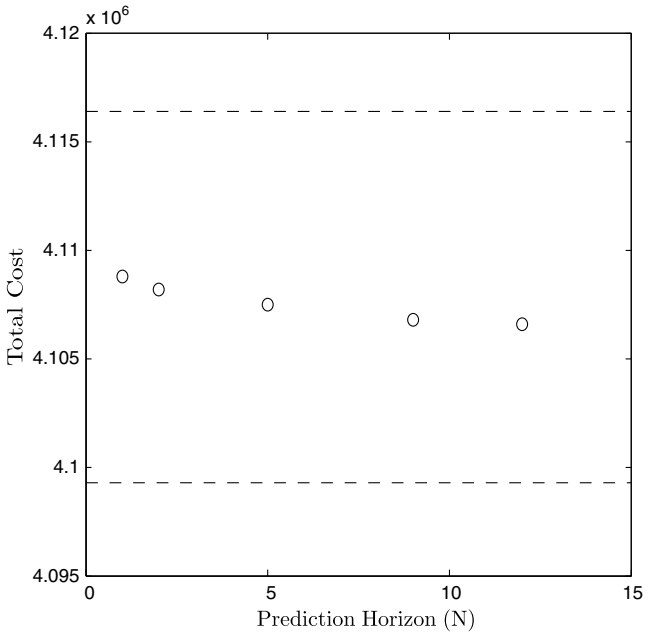

Fig. 10. Total optimization cost vs. prediction horizon with upper and lower bounds based on maximum transition speed.

tion, the MPC controlled cases should perform better than the maximum speed transition (again, the "open-loop manually controlled" case) where the pressure is weighted equivalently to the MPC controlled cases. It can be seen in Fig. 10 that all of the MPC controlled cases at various prediction horizons fall between these two bounds. It is also noted that the magnitudes of the cost function values depend on the individual weighting on each term, but the trend will be independent of term weighting.

4.3. Optimal mode transition with plant-model mismatch on feed quality

In order to evaluate the effectiveness of the MPC in the presence of a disturbance, a plant-model mismatch was imposed on the feed TDS value. In these simulations, the MPC algorithm continues to use the nominal feed TDS value of 10,000 ppm, while the plant simulation is conducted using the true feed value of 9000 ppm.

It can be seen in Fig. 11 that this plant-model mismatch results in a sizeable pressure offset from the original set point. This offset is due to the fact that the controller is using the nominal feed TDS value in its calculations instead of the actual plant value. An offset can be observed in the velocity and control action plots as well (Figs. 12, 13), but to a lesser degree. The amount of offset also changes when the prediction horizon is varied, due to the increased performance of the optimization algorithm when the prediction horizon is increased. If it is necessary to bring the system pressure back to the nominal set point, integral control can be ap-

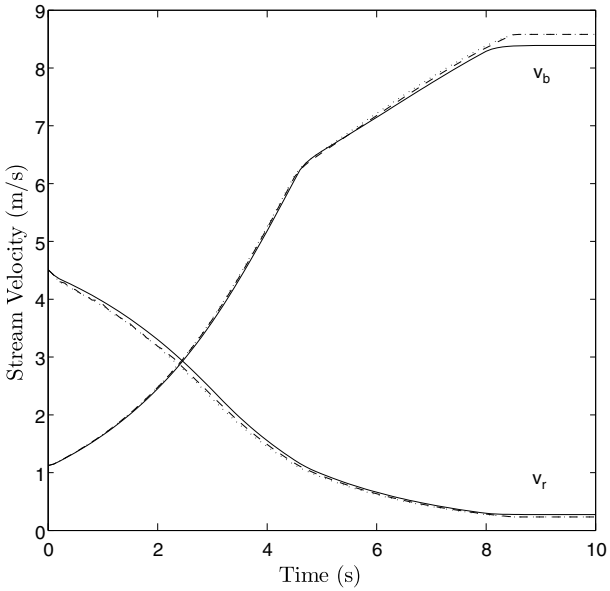

Fig. 12. Steady-state switching using MPC in the presence of plant-model mismatch on feed TDS: stream velocities vs. time for $N = 1$ (solid line), $N = 3$ (dashed line), and $N = 5$ (dotted line).

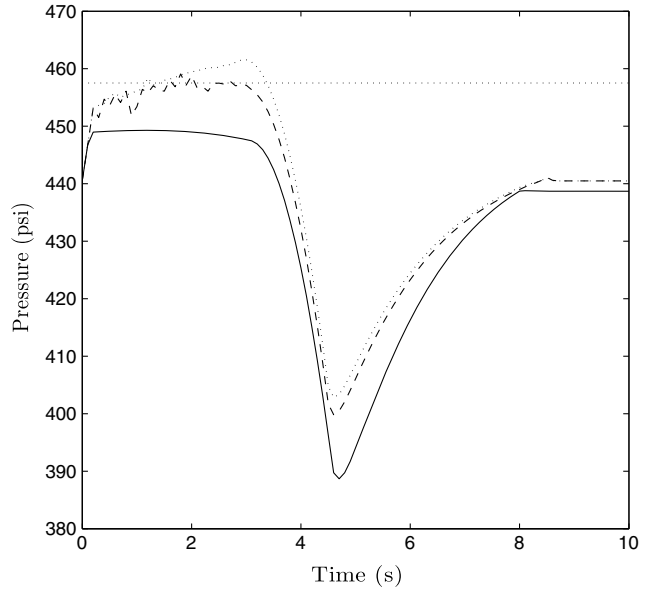

Fig. 11. Steady-state switching using MPC in the presence of plant-model mismatch on feed TDS: system pressure vs. time for $N = 1$ (solid line), $N = 3$ (dashed line), and $N = 5$ (dotted line), including pressure set point (horizontal line).

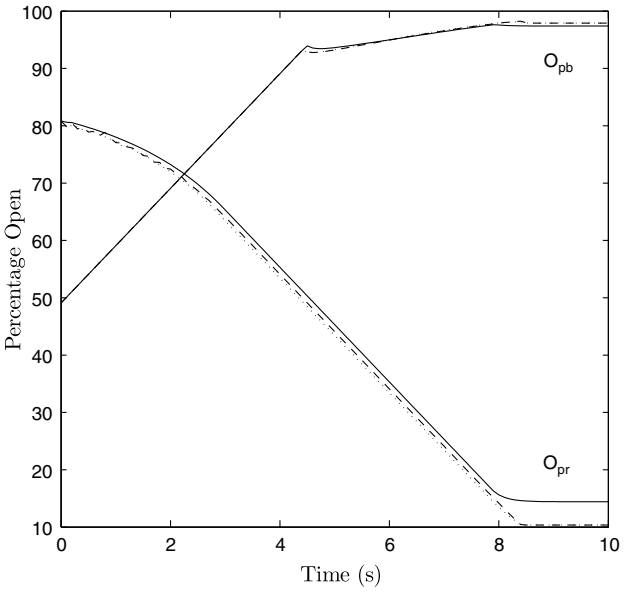

Fig. 13. Steady-state switching using MPC in the presence of plant-model mismatch on feed TDS: valve positions vs. time for $N = 1$ (solid line), $N = 3$ (dashed line), and $N = 5$ (dotted line).

plied to the system after the MPC has finished acting. This integral term can be implemented in the following two ways: First,

$$u^r_{\text{total}} = u^{\text{rf}}_{\text{MPC}} + \frac{1}{\tau^r_i}\int_{10}^{t_c}(P_{\text{sys}} - P^{\text{sp}}_{\text{sys}})\mathrm{d}t \tag{15}$$

where $u^{\text{rf}}_{\text{MPC}}$ represents the final value for the MPC retentate valve control action after reaching the steady-state determined by the optimization, t_c is the current time, and $(P_{\text{sys}} - P^{\text{sp}}_{\text{sys}})$ is the error between the actual system pressure and the nominal set point pressure, and τ^r_i is the integral time constant ($\tau^r_i = 10$). Second,

$$u^b_{\text{total}} = u^{\text{bf}}_{\text{MPC}} + \frac{1}{\tau^b_i}\int_{10}^{t_c}(v_{\text{b}} - v^{\text{lss}}_{\text{b}})\mathrm{d}t \tag{16}$$

where $u^{\text{bf}}_{\text{MPC}}$ represents the final value for the MPC bypass valve control action after reaching the steady-state determined by the optimization, $(v_{\text{b}} - v^{\text{lss}}_{\text{b}})$ is the error between the actual bypass velocity and the low-flow steady-state bypass velocity, and τ^b_i is the integral time constant ($\tau^b_i = \frac{1}{30}$).

In the results presented in Figs. 14–16, it is seen that the MPC optimization reaches a steady-state around $t = 8$ s; after this steady-state is reached, the MPC is deactivated and the integral control is initiated at $t = 10$ s. In both cases, the offsets are eliminated; the offset on pressure is eliminated in the case of the integral term using pressure measurements, and the offset on bypass velocity is eliminated in the second case. It can also be observed that the system pressure deviates even more than the original offset in

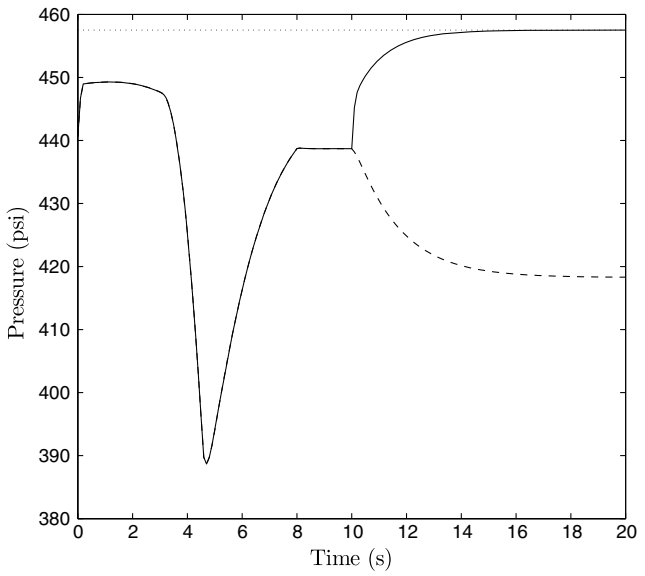

Fig. 14. Mode transition using MPC and integral control in the presence of plant-model mismatch on feed TDS: system pressure vs. time for integral term based on system pressure (solid line) and integral term based on bypass velocity (dashed line) with pressure set point (dotted line) for $N = 1$.

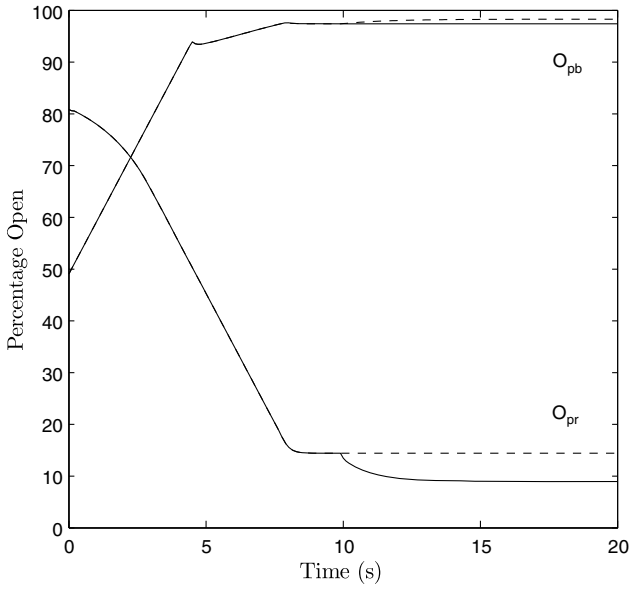

Fig. 16. Mode transition using MPC and integral control in the presence of plant-model mismatch on feed TDS: valve positions vs. time for integral term based on system pressure (solid lines) and integral term based on bypass velocity (dashed lines) for $N = 1$.

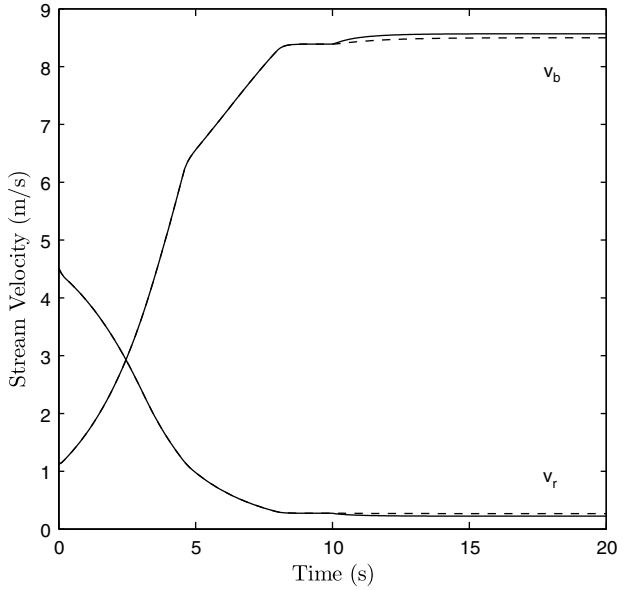

Fig. 15. Mode transition using MPC and integral control in the presence of plant-model mismatch on feed TDS: bypass and retentate stream velocities vs. time for integral term based on system pressure (solid lines) and integral term based on bypass velocity (dashed lines) for $N = 1$.

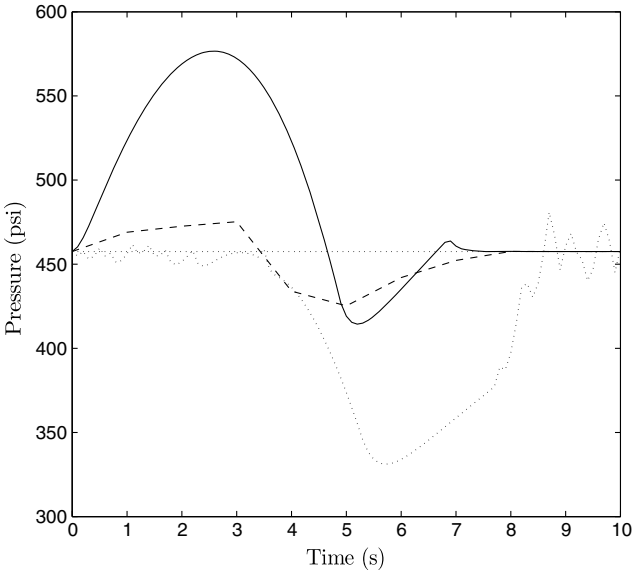

Fig. 17. Mode transition using MPC in the absence of plant-model mismatch: system pressure vs. time for algebraic steady-state MPC formulation (dashed line), "open-loop manually controlled" case (solid line), and first PI approach (dotted line).

the case where the integral term is based on the bypass velocity. Other methods may be used to correct for MPC offset due to plant-model mismatch; the approach followed here is only one example. For more detailed information on PI controller tuning, see [12].

4.4. Use of steady-state process model in MPC

Finally, the issue of reduction of the time needed to compute the control action by MPC is investigated. Specifically, motivated by the fast time-scale of the RO system dynamics, an algebraic steady-state approximation of the model equations is used in place of the dynamic model in the MPC formulation. In this case, the MPC algorithm with a prediction horizon $N = 1$ takes the form:

$$
\begin{aligned}
&\min_{e_{vb},e_{vr}} \sum_{i=n_c}^{n_c+1} \left[\alpha \left(\frac{P_{sys}(i)}{P_{sys}^{sp}} - 1 \right)^2 + \beta \left(\frac{v_{fr}(i)}{v_{wh}} - 1 \right)^2 + \gamma \left(\left(\frac{e_{vb}(i)}{e_{vb}^{lss}} - 1 \right)^2 + \left(\frac{e_{vr}(i)}{e_{vr}^{lss}} - 1 \right)^2 \right) \right] \\
&0 = \frac{A_p^2}{A_m K_m V}(v_f - v_b - v_r) + \frac{A_p}{\rho V}\Delta\pi - \frac{1}{2}\frac{A_p e_{vb} v_b^2}{V} \\
&0 = \frac{A_p^2}{A_m K_m V}(v_f - v_b - v_r) + \frac{A_p}{\rho V}\Delta\pi - \frac{1}{2}\frac{A_p e_{vr} v_r^2}{V} \\
&O_{pi} \geqslant 0, \left| \frac{dO_{pi}}{dt} \right| \leqslant R_{valve}^{max} \\
&\Delta\pi = \delta C_{eff}(T + 273), C_{eff} = C_{feed}\left(a + (1 - a)\left(\frac{(1 - R) + R(v_f - v_b)}{v_r} \right) \right) \\
&P_{sys} = \frac{\rho A_p}{A_m K_m}(v_f - v_b - v_r) + \Delta\pi
\end{aligned}
\tag{17}
$$

In the stream velocity and control action plots (Figs. 18 and 19), it is seen that the algebraic steady-state MPC formulation is very similar to the "open-loop manually controlled" case, but the small differences in control action have a large effect on the system pressure. A large fluctuation in system pressure can be observed in Fig. 17, showing that even with a larger sampling time, a prediction horizon of one, and only using steady-state algebraic equations in the optimization algorithm, the MPC formulation still performs much better than the "open-loop manually controlled" case. As expected, the steady-state MPC formulation does not perform as well as the closed-loop system using the MPC with dynamic model equations. In terms of computation time, it was found that the steady-state algebraic MPC formulation and the MPC formulation using the dynamic model computed the optimal control actions in approximately the same amount of time (for any given prediction horizon). The steady-state algebraic MPC formulation of Eq. (17) is slightly faster in terms of computation time relative to the MPC with the dynamic process model, but the benefits of increased

In Figs. 17–19, the closed-loop system results (under the MPC) using the steady-state algebraic equations with a sampling time of 1 s are presented and compared to the "open-loop manually controlled" case (where the valves are opened to their final steady-state at the maximum rate allowed).

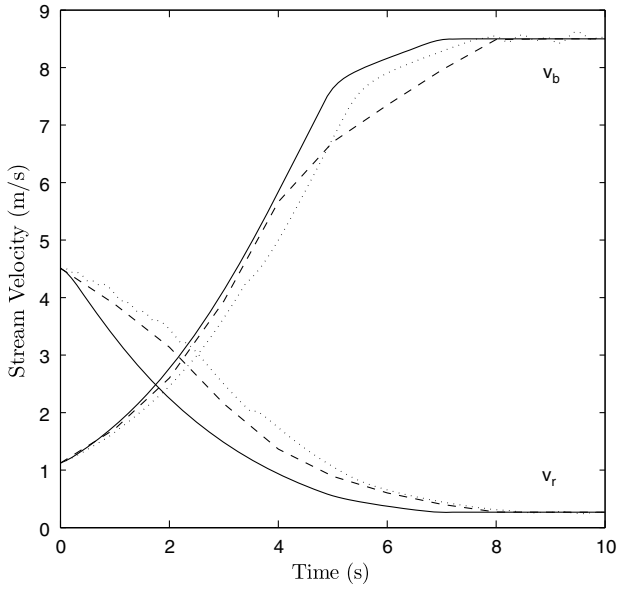

Fig. 18. Mode transition using MPC in the absence of plant-model mismatch: stream velocities vs. time for algebraic steady-state MPC formulation (dashed line), "open-loop manually controlled" case (solid line), and first PI approach (dotted line).

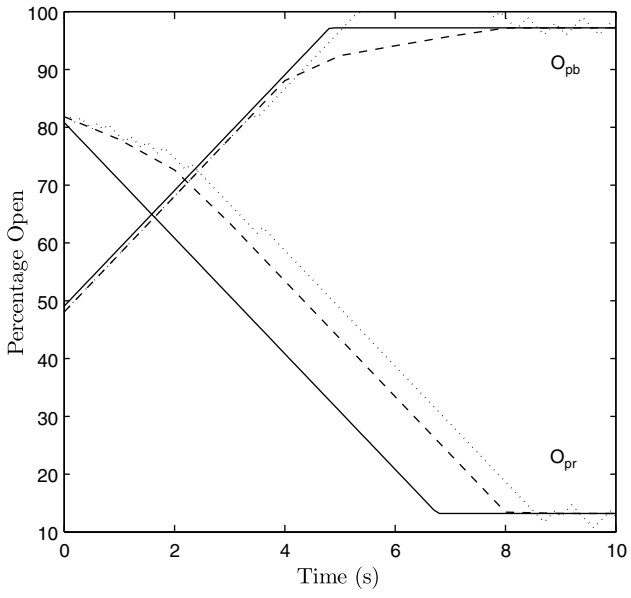

Fig. 19. Mode transition using MPC in the absence of plant-model mismatch: valve positions vs. time for algebraic steady-state MPC formulation (dashed line), "open-loop manually controlled" case (solid line), and first PI approach (dotted line).

performance in the dynamic formulation far outweigh this discrepancy in computation time. This result demonstrates that the majority of computation time is used to perform the optimization, and not to perform the integration of the dynamic system model in the controller. Overall, it is more beneficial to use the dynamic model in the closed-loop MPC algorithm with a dedicated processor to carry out the calculations.

5. Conclusions

In this work, a model-predictive control strategy for switching between the normal flow operating steady-state and the feed flow reversal steady state (where flow into the membrane units is low enough to prevent water hammer when solenoid valves are closed) was developed. First, a dynamic model of the process was developed as a function of the process parameters, feed concentration, and the bypass/retentate valve resistance values. Using these valve resistance values as control inputs, a non-linear optimization problem was formulated. Solving this optimization through a model-predictive control framework, it was seen that a feedback-based controller allowed the system to make the transition between steady-states with a much smaller variation in system pressure. The MPC framework was also shown to have smaller pressure fluctuations and shorter transition time than several well-tuned PI controllers. Non-linear MPC was also shown to be beneficial in the presence of plant-model mismatch. The feedback-based MPC algorithm also improved the speed at which the stream velocities reached the feed flow reversal steady-state, decreased the offset between the actual final steady-state and the desired final steady-state, and damped oscillations in the control action. It was also demonstrated that the benefits of using the dynamic MPC formulation to provide increased system performance outweighed the slightly decreased computation time of using the MPC with a steady-state process model.

Acknowledgement

Financial support from the National Science Foundation, CTS-0529295, and the State of California Department of Water Resources is gratefully acknowledged.

References

[1] A. Abbas, Model-predictive control of a reverse osmosis desalination unit, Desalination 194 (2006) 268–280.
[2] R.B. Bird, W.E. Stewart, E.N. Lightfoot, Transport Phenomena, second ed., John Wiley and Sons, 2002. pp. 203–206.
[3] F.H. Butt, F. Rahman, U. Baduruthamal, Identification of scale deposits through membrane autopsy, Desalination 101 (1995) 219–230.
[4] P.D. Christofides, N.H. El-Farra, Control of Nonlinear and Hybrid Process Systems: Designs for Uncertainty, Constraints and Time-Delays, Springer, New York, 2005. 446 p.
[5] N.H. El-Farra, P. Mhaskar, P.D. Christofides, Hybrid-predictive control of nonlinear systems: Method and applications to chemical processes, Inter. J. Rob. Nonlinear Contr. 14 (2004) 199–225.
[6] S. Hargrove, S. Ilias, Flux enhancement using flow reversal in ultrafiltration, Separ. Sci. Technol. 34 (1999) 1319–1331.
[7] D. Hasson, A. Drak, R. Semiat, Inception of CaSO4 scaling on RO membranes at various water recovery levels, Desalination 139 (2001) 73–81.
[8] R.A. Leishear, Dynamic pipe stresses during water hammer: A finite element approach, J. Pressure Vessel Technol. 129 (2007) 226–233.
[9] Y. Lu, Y. Hu, X. Zhang, L. Wu, Q. Liu, Optimum design of reverse osmosis system under different feed concentration and product specification, J. Membr. Sci. 287 (2007) 219–229.
[10] C.W. McFall, P.D. Christofides, Y. Cohen, J.F. Davis, Fault-tolerant control of a reverse osmosis desalination process, in: Proceedings of 8th IFAC Symposium on Dynamics and Control of Process Systems, vol. 3, Cancun, Mexico, 2007, pp. 163–168.
[11] C.W. McFall, A.R. Bartman, P.D. Christofides, Y. Cohen, Control of a reverse osmosis desalination process at high recovery, Ind. Eng. Chem. Res., in press.
[12] P. Mhaskar, N.H. El-Farra, P.D. Christofides, A framework for classical controller tuning using nonlinear control techniques, AIChE J. 51 (2005) 3292–3299.
[13] P. Mhaskar, N.H. El-Farra, P.D. Christofides, Predictive control of switched nonlinear systems with scheduled mode transitions, IEEE Trans. Automat. Contr. 50 (2005) 1670–1680.
[14] P. Mhaskar, N.H. El-Farra, P.D. Christofides, Stabilization of nonlinear systems with state and control constraints using Lyapunov-based-predictive control, Syst. Contr. Lett. 55 (2006) 650–659.
[15] R.H. Perry, D.W. Green, Perry's Chemical Engineers' Handbook, seventh ed., McGraw-Hill, 1997. pp. 6–44.
[16] N. Pomerantz, Y. Ladizhansky, E. Korin, M. Waisman, N. Daltrophe, J. Gilron, Prevention of scaling of reverse osmosis membranes by "zeroing" the elapsed nucleation time. part i. calcium sulfate, Ind. Eng. Chem. Res. 45 (2006) 2008–2016.
[17] A. Rahardianto, J. Gao, C.J. Gabelich, M.D. Williams, Y. Cohen, High recovery membrane desalting of low-salinity brackish water: Integration of accelerated precipitation softening with membrane RO, J. Membr. Sci. 289 (2007) 123–137.
[18] A. Rahardianto, W. Shih, R. Lee, Y. Cohen, Diagnostic characterization of gypsum scale formation and control in RO membrane desalination of brackish water, J. Membr. Sci. 279 (2006) 655–668.
[19] M. Uchymiak, A. Rahardianto, E. Lyster, J. Glater, Y. Cohen, A novel RO ex situ scale observation detector (EXSOD) for mineral scale characterization and early detection, J. Membr. Sci. 291 (2007) 86–95.